CHEMISTRY
A EUROPEAN JOURNAL

DOI: 10.1002/chem.200801611

Macrocyclic Cyclooctene-Supported AlCl–Salen Catalysts for Conjugated Addition Reactions: Effect of Linker and Support Structure on Catalysis

Nandita Madhavan,[b] Tait Takatani,[b] C. David Sherrill,[b] and Marcus Weck*[a, b]

Abstract: AlCl–salen (salen = *N*,*N*′-bis(salicylidene)ethylenediamine dianion) catalysts supported onto macrocyclic oligomeric cyclooctene through linkers of varying length and flexibility have been developed to demonstrate the importance of support architecture on catalyst activity. The role played by the support and the linkers in dictating catalyst activity was found to vary for reactions with contrasting mechanisms, such as the bimetallic cyanide and the monometallic indole addition reactions. While the flexible support significantly enhanced the cyanide addition reaction, most likely by improving salen–salen interactions in the transition state, it lowered the reaction rate for the monometallic indole reaction. For both reactions, significant increase in catalytic activity was observed for catalysts with the longest linkers. The effect of the flexible macrocyclic support on catalysis was further exemplified by the enhanced activity of the supported catalyst in comparison with its unsupported analogue for the conjugate addition of tetrazoles, which is known to be catalyzed by dimeric μ-oxo–salen catalysts. Our studies with the cyclooctene supported AlCl–salen catalysts provides significant insights for rationally designing highly efficient AlCl–salen catalysts for a diverse set of reactions.

Keywords: aluminum · asymmetric catalysis · conjugated addition · N,O ligands · ROMP (ring-opening metathesis polymerization) · supported catalysts

Introduction

Organometallic salen (salen = *N*,*N*′-bis(salicylidene)ethylenediamine dianion) catalysts have emerged as powerful tools in facilitating the synthesis of important materials and therapeutic agents. Environmental concerns associated with the disposal of such catalysts, coupled with financial concerns due to their increasing costs, have led to considerable research focused towards the development of green and economically viable alternatives such as supported metal–salen catalysts.[1–5] Several supports ranging from high-molecular-weight polymers and inorganic supports to dendrimers and oligomers have been explored for salen complexes.[1,6–11] The high-molecular-weight supports typically facilitate the easy recovery and reuse of catalysts, whereas the low-molecular-weight supports are often designed to enhance the catalytic activity of the supported catalysts in comparison with their non-supported analogues. While there has been significant advancement in the development of recoverable catalysts,[1–3] there have been limited efforts correlating the effect of support architecture to the activity of the catalyst.[12]

In general, immobilized catalysts have three components: a support material, such as a polymer or a surface, a catalyst, and a linker connecting the two. The nature of the linker and the support material can have a profound effect on the activity of the catalyst. Extremely high catalytic activities have been observed for catalysts with dimeric, oligomeric, and dendritic supports for the bimetallic Co–salen-catalyzed reactions, due to an increased local concentration of catalysts on the support.[6,10,11,13] In contrast, for the monometallic Mn–salen-catalyzed epoxidation reaction, supports with lower local concentration of catalysts have been found to enhance the reactivity.[7,14–16] Furthermore, longer and flexible linkers have been demonstrated to improve both the bimetallic Co–salen hydrolytic kinetic resolution (HKR) reaction as well as the monometallic Mn–salen epoxidation reaction.[17–19] Another class of metal–salen catalysts, Al–salen complexes, are known to catalyze industrially impor-

[a] Prof. Dr. M. Weck
Molecular Design Institute and Department of Chemistry
New York University, New York, NY 10003 (USA)
Fax: (+1) 212-995-4895
E-mail: marcus.weck@nyu.edu

[b] Dr. N. Madhavan, T. Takatani, Prof. Dr. C. D. Sherrill, Prof. Dr. M. Weck
School of Chemistry and Biochemistry
Georgia Institute of Technology, Atlanta, GA 30332 (USA)

Supporting information for this article is available on the WWW under http://dx.doi.org/10.1002/chem.200801611.

tant conjugate addition reactions, some of which are hypothesized to follow a bimetallic pathway,[20,21] while others presumably follow a monometallic pathway.[22] Hence, Al–salen complexes are a perfect system to study the effect of support structure and linker length on the catalysis of mono- and bimetallic reactions and to verify the proposed guidelines in the literature of supported catalyst design.[12] Despite this fact, there are only two studies reported in the literature pertaining to the design of supported Al–salen catalysts[23,24] and only one of them is pertinent to conjugate addition reactions.[23] Herein, we introduce macrocyclic cyclooctene-supported, AlCl–salen catalysts to study the importance of catalyst structure on the conjugate addition of nucleophiles to α,β-unsaturated imides and ketones (Figure 1).

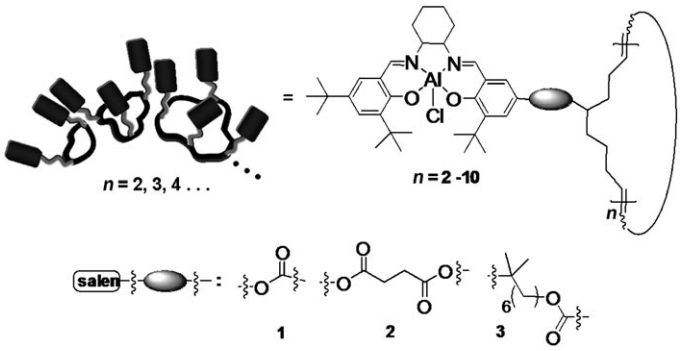

Figure 1. Supported (salen)AlCl catalysts attached to oligomeric cyclooctene macrocycle through varied linkers.

Our investigations are the first to compare and contrast the effect of support architecture on mono- and bimetallic AlCl–salen-catalyzed reactions. We demonstrate that a flexible support significantly enhances the bimetallic reaction and lowers the reaction rate for the monometallic reaction, while longer linkers increase the catalytic activity for both reactions.

Our catalyst design utilizes the oligomeric cyclooctene macrocycle as the backbone support, which is readily obtained by the ring-opening metathesis polymerization (ROMP) of cyclooctene-derived monomers under dilute conditions.[25,26] The dramatic enhancements shown by the macrocyclic cyclooctene backbone with Co–salen[10] makes it an ideal candidate to study the catalysis of the bimetallic AlCl–salen-catalyzed cyanide addition to α,β-unsaturated imides. The flexible cyclooctene support is also a good example to investigate whether the increased local concentration of AlCl–salen complexes on the support has a detrimental effect on the catalysis of a reaction that involves a monometallic transition state including the addition of indole to α,β-unsaturated ketones. To investigate the effect of linker length and flexibility on the catalytic activity, the AlCl–salen complexes were attached to the macrocyclic backbone by using three different linkers as illustrated in Figure 1. The linkers vary in length and flexibility with catalyst **1** having the shortest linker resulting in the least flexible side-chain, catalyst **2** having a medium-sized linker with moderate flexibility, while catalyst **3** is based on the longest and most flexible linker.

Results and Discussion

The oligomeric catalysts **1**–**3** can be synthesized readily in high yields from commercially available starting materials. Catalysts **1** and **2** were synthesized from the reaction of salen ligand **4** with cyclooctene carboxylic acids **5** or **6** via the intermediates **7**–**10** (Scheme 1). Catalyst **3** was synthesized from ligand **11**[23] (Scheme 2). The salen ligands **4** and **11** were readily obtained from cyclohexane monohydrochloride salt by the one-pot synthesis of unsymmetrical salens developed by our group.[27] The ligands were coupled with cyclooctene carboxylic acids in the presence of dicyclohexylcarbodiimide (DCC) and 4-(dimethylamino)pyridine (DMAP) to afford the corresponding unmetalated monomers (**7**, **8**, and **12**) in high yields. Solutions of monomers **7**, **8**, and **12** at concentrations of 0.1 M in dichloromethane were subjected to ROMP using Grubbs' third-generation initiator to afford the cyclic oligomers **9**, **10**, and **13**, respectively. The formation of the macrocycles was confirmed by ^{1}H NMR spectroscopy, gel-permeation chromatography, and mass spectrometry. ^{1}H NMR spectroscopy indicated the absence of end-group signals, while GPC data showed the formation of lower molecular weight oligomeric species. MALDI-TOF mass spectrometry provided direct evidence for the formation of the cyclic structures as signals corresponding to macrocycles of different sizes with values of "*n*" ranging from two to ten were observed. These results are in close analogy to our recent reported cyclooctene-based Co–salen macrocycles.[10] The cyclic oligomers were then subjected to metalation by addition of a solution of diethyl aluminum chloride to afford catalysts **1**–**3** in 90–99% yields. Complete metalation was confirmed by the disappearance of the phenolic protons in the ^{1}H NMR spectrum of the catalysts and the aluminum ICP elemental analyses of the catalysts.[28]

The activity of the catalysts was first assessed for the asymmetric addition of cyanide to α,β-unsaturated imide **14**, which has been reported to follow second-order kinetics with respect to the catalyst (Table 1).[20,21] The cyanide was generated in situ from isopropanol and trimethylsilyl cyanide in the presence of the imide **14** and the catalyst in toluene at 45 °C. The reactions were sealed to minimize cyanide leakage, which prevented the evaluation of the reaction progress by thin-layer chromatography. Therefore, the reaction with each catalyst was carried out for a time period of 18 h, following which the yield of the isolated product **15** was determined to compare the efficiency of the catalyst.[29] Table 1 illustrates the yields and enantioselectivities for **15** using the catalysts **1**–**3**.

The nature of the linker played an important role in dictating the yields and enantioselectivities of **15**. Lower yields (70%) were obtained with **1**, which had the shortest and most rigid linker, with respect to **2** and **3** with the medium

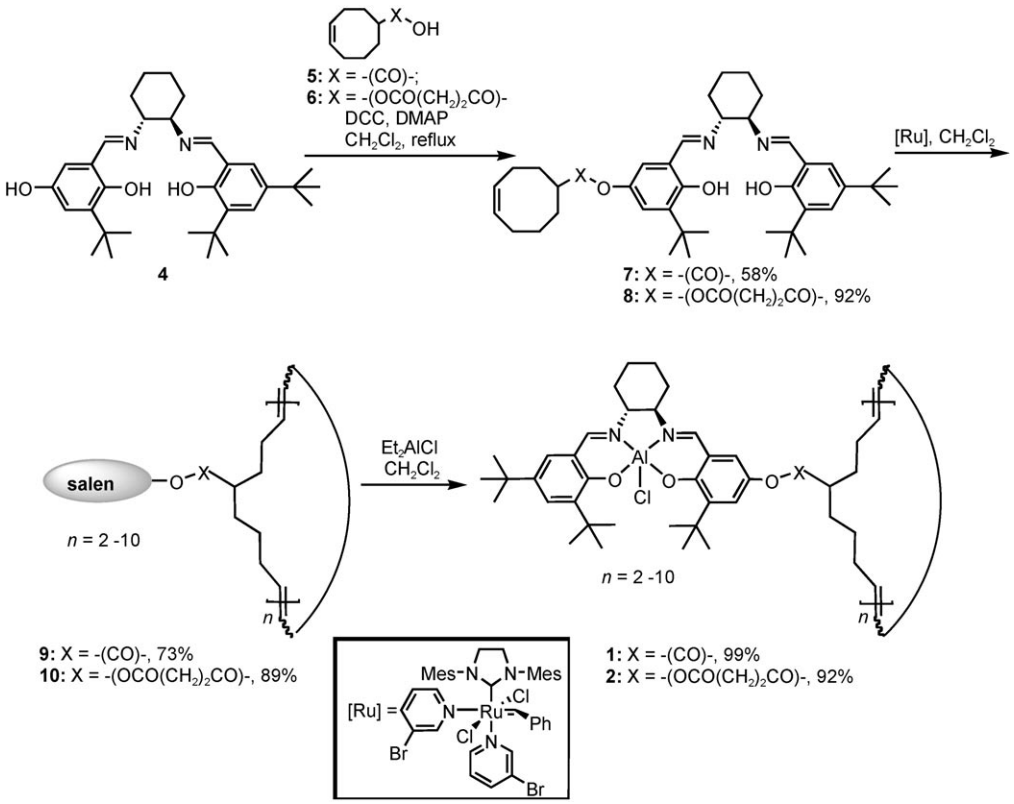

Scheme 1. Synthetic pathway to obtain catalysts **1** and **2**.

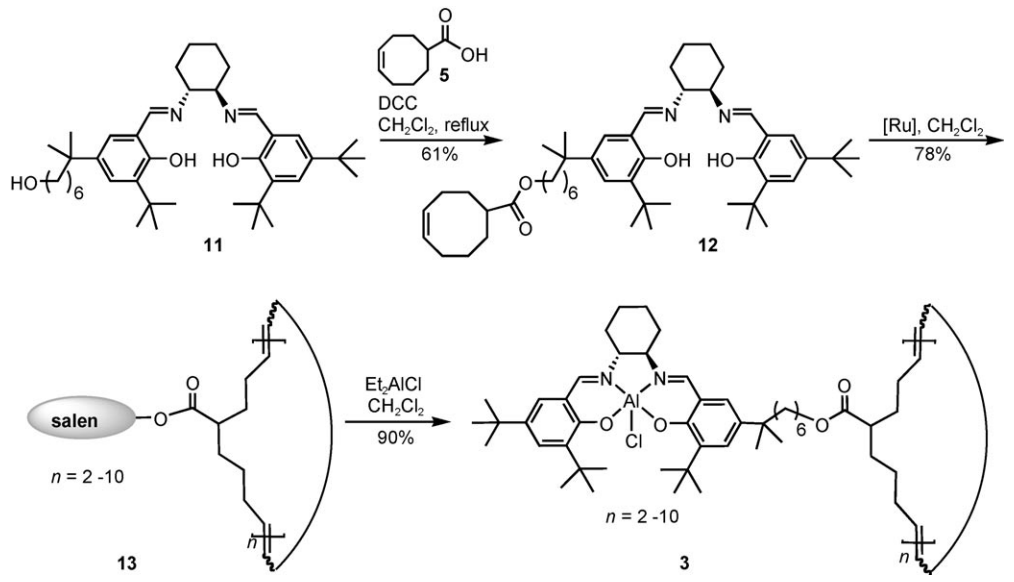

Scheme 2. Synthetic route for catalyst **3**.

and long linkers, respectively. The improved yields of **15** with an increase in the length and flexibility of the linker suggests that a more flexible linker makes the interaction between the two catalytic AlCl–salen centers that form the bimetallic transition state more facile. The enantioselectivities of the products also depended on the structure of the catalyst. Catalyst **3** in which the linker was attached to the salen through a tertiary carbon atom gave the best enantiomeric excesses (*ee*'*s*) in comparison to **2** and **1**. Surprisingly, the *ee* of **15** obtained with **2** was slightly lower than that obtained with **1**. In all cases, the yields obtained for adduct **15** using the cyclooctene catalysts were superior to the yields obtained with the Jacobsen AlCl–salen catalyst (<20%) under the same reaction conditions.[23] The higher yields sug-

Table 1. Effect of linker on yield and selectivity of the bimetallic cyanide addition.

	Catalyst	Yield[a] [%]	*ee* [%][b]
1	**1** (short)	70	93
2	**2** (medium)	94	82
3	**3** (long)	98	98

[a] Isolated yield. [b] Enantiomeric excess determined by HPLC analysis using a chiral Pirkle-L-leucine column.

gest that the macrocyclic support does indeed play a significant role in enhancing the reaction. The most notable fact was that a 50% lower catalyst loading (5 mol%) than that reported for the unsupported AlCl–salen catalyst was used, indicating the importance of the nature of the support on the catalysis.[20] The initial rates of the most active cyclooctene catalyst **3** and the unsupported catalyst were compared by using ^{1}H NMR spectroscopy. The kinetics were studied by setting up the cyanide addition reaction in five NMR tubes and quenching each reaction at different time periods. Conversions were determined by comparing the areas obtained upon the integration of the product peaks with that for 1,1,2,2-tetrachloroethane, which was used as an internal standard.

For **3**, the reaction was 80% complete within 8 h, while the Jacobsen catalyst showed less than 20% conversion after 6 h. The kinetics data indicate that the activity of **3** is significantly higher than that for the unsupported Jacobsen (AlCl) catalyst, most likely due to the bimetallic nature of the catalysis and the enhanced proximity of two metal sites due to the support structure as well as the flexibility of the support and the linker (Figure 2). To ensure that the difference in catalytic activities between **1–3** were not due to changes in the electronic properties of the catalytic center, B3LYP/6–31G* computational studies were carried out to determine the atomic charges on the ligand and the aluminum in the presence of the linkers.[30] The results as illustrated in Table 2 indicate that the atomic charges on the atoms do not vary with the nature of the linker.

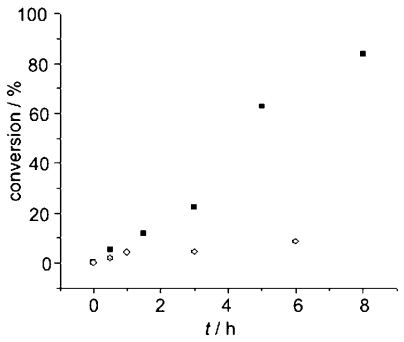

Figure 2. Effect of support on catalytic activity: comparison of initial rates of **3** (■) with the non-supported Jacobsen catalyst (◇).

Table 2. B3LYP/6-31G* atomic charges on the atoms in the catalytic center.

Linker	Al	N	N	O	O	Cl
short	0.53	−0.30	−0.21	−0.25	−0.33	−0.39
medium	0.52	−0.30	−0.21	−0.24	−0.33	−0.39
long	0.53	−0.29	−0.23	−0.26	−0.33	−0.39

After establishing the positive effect of the macrocyclic support on the bimetallic cyanide addition reaction, we wished to investigate if the increased local concentration of the catalyst on the support would lead to lower activities for a monometallic reaction. Therefore, the activity of **1** and **3**[31] were studied for the addition of indole **17** to the α,β-unsaturated ketone **16**,[32] which was reported to follow a monometallic pathway in the literature.[22,33] The reactions were carried out in toluene for 18 h and the yields for the product were determined after purification by using flash column chromatography.

As illustrated in Table 3, lower yields and *ee*'s were observed for the product obtained when catalyst **1** was used. The lower yields and *ee*'s indicated that the increased

Table 3. Effect of linker on yield and enantioselectivity of monometallic indole addition reaction.

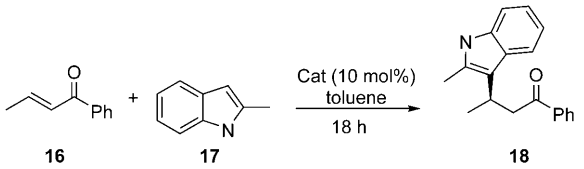

	Catalyst	Yield[a] [%]	*ee* [%][b]
1	Jacobsen Catalyst	81	37
2	**1** (short)	65	26
3	**3** (long)	92	24

[a] Isolated yield. [b] Enantiomeric excess determined by HPLC analysis using a chiralcel OD column.

crowding of catalysts on the cyclooctene support did indeed lower the catalytic activity. A similar effect for the selectivities and conversions has been observed with Mn–salen systems for the monometallic asymmetric epoxidation reaction.[7] The lower selectivities might be attributed to the difficulty of the reagents in accessing the catalytic site due to excessive crowding. While the selectivities remained low for adduct **18** obtained with **3**, the yields were significantly improved and even higher than that obtained with the unsupported catalyst. We believe this intriguing increase in yield is a result of the greater solubility of **3** in comparison to **1** and the unsupported catalyst in the reaction medium due to the presence of the long hydrophobic alkyl chains. To prove this hypothesis, the reactions were carried out in a reaction medium, such as methylene chloride, in which all the cata-

lysts are highly soluble; comparable rates were obtained for all catalysts. Based on our observations with the indole addition reaction, we hypothesize that the detrimental effects of the support are not very pronounced and could be offset by an increased solubility of the catalyst as observed with **3**.

The rates for the catalysis of the indole addition reaction by **1**, **3**, and the unsupported catalyst were determined by using ^{1}H NMR spectroscopy and their activities were compared (Figure 3). The kinetics were studied by setting up the

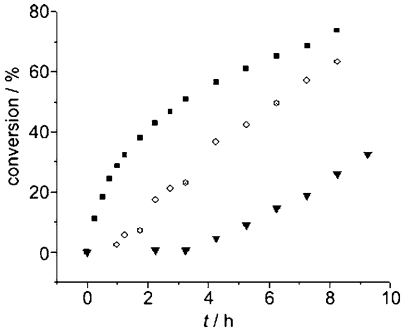

Figure 3. Comparison of initial rates for the indole addition reaction. Jacobsen catalyst: ◇; catalyst **1**: ▼, catalyst **3**: ■.

reactions in [D_8]toluene in NMR tubes in the presence of an internal standard, such as 1,1,2,2-tetrachloroethane. NMR spectra were obtained at different time intervals in order to determine the conversions. The initial rate for the reaction catalyzed by **3** is significantly higher than that with **1** and the Jacobsen catalyst as evidenced by greater than 50% conversions within 2.5 h. The pronounced difference in the activities of **1** and **3** illustrates that for this monometallic reaction, the hydrophobicity of the linker plays a more important role than its flexibility in improving catalysis.

The studies with the indole and cyanide addition reaction indicated that **3** was the most active catalyst among the oligomeric-cyclooctene-supported Al–salen systems. After investigating the support and linker effects, we wished to study if the close proximity of the AlCl–salen on our cyclooctene backbone in **3** could be exploited for reactions such as the addition of tetrazole **19** to α,β-unsaturated ketones and imides that have been catalyzed by the dimeric μ-oxo–Al–salen catalyst.[34] Since, the mechanism of the tetrazole addition has not been reported, we were uncertain if the steric and electronic differences between AlCl–salen and the dimeric oxo–salen catalysts would affect the yields and selectivities of the product. The reaction with the dimeric salen catalyst has been reported at room temperature with 5 mol% of catalyst (10 mol% with respect to Al). With the Jacobsen AlCl–salen catalyst as well as **3**, we observed that elevated temperatures of 55°C were necessary to facilitate the reaction and little or no selectivities were observed, indicating that an AlCl–salen catalyst might not be the ideal catalyst for this transformation. Despite the low *ee*'s, we were keen on studying the effect of the macrocyclic support on the catalysis and set out to compare the difference in catalytic activity of **3** and its unsupported AlCl–salen analogue (Table 4). The yields for the formation of the adduct **20** were found to be higher when **3** was employed, with the difference being more pronounced for the reaction with imide **14** than with ketone **16**. It was notable that high yields were obtained with only 5 mol% of the catalyst, which again is a 50% lower loading than that of the dimeric μ-oxo–salen catalyst. In the case of imide **14**, the loading could be lowered even further by 50% (2.5 mol%) without significantly compromising the yield of the adduct **20b**.

Table 4. Conjugate addition of 5-phenyltetrazole to α,β-unsaturated ketones and imides.

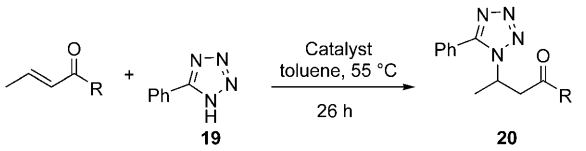

19 **20**

	R	Catalyst	Loading [mol%]	Yield [%][a]
1	**16**: Ph	Jacobsen catalyst	5	**20a**: 73
2	**16**: Ph	**3** (long)	5	**20a**: 91
3	**14**: -NHCOPh	Jacobsen catalyst	5	**20b**: 74
4	**14**: -NHCOPh	**3** (long)	5	**20b**: 98
5	**14**: -NHCOPh	**3** (long)	2.5	**20b**: 85

[a] Isolated yield.

To understand the magnitude of difference in the activities of **3** and the unsupported catalyst, we monitored the reaction kinetics by using ^{1}H NMR spectroscopy in the presence of 1,1,2,2-tetrachloroethane as an internal standard (Figure 4). In all cases the reaction progressed significantly faster with **3** when compared to Jacobsen catalyst. For the addition to imide **14**, the differences in rates were more pronounced; the conversion to the product **20b** was observed in less than 10 h with 5 mol% of **3**. The activity with 2.5 mol% catalyst, although lower than that with 5 mol% **3**, was still higher than that for 5 mol% of the unsupported Jacobsen catalyst. The enhancement of catalytic activity by virtue of the flexibility of the macrocyclic backbone exemplifies the crucial role of flexible supports on the reaction catalysis. Studies are currently ongoing to incorporate the lessons learnt from the macrocyclic backbone into the development other supported catalysts that show not only enhanced reactivities, but also good selectivities for the addition of nucleophiles such as tetrazoles.

Conclusion

We have used AlCl–salen catalysts attached to oligomeric macrocyclic cyclooctene supports by varied linkers as model systems to study the effect of linker and support on bi- and monometallic conjugate addition reactions. The flexibility and ability of the cyclooctene support to enhance interaction between neighboring AlCl–salen units makes the catalysts superior to their unsupported analogues for the bimetallic

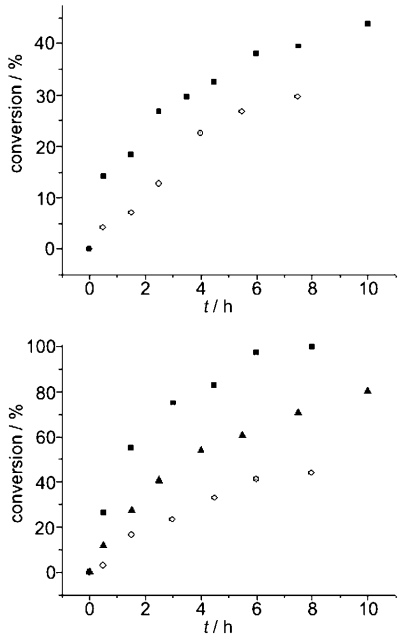

Figure 4. Comparison of initial rates for the addition of tetrazole **17** to α,β-unsaturated ketones (top) and imides (bottom) between catalyst **3** and unsupported Jacobsen AlCl–salen catalyst. Top: Catalyst **3**: ■; Jacobsen: ◇; Bottom: Catalyst **3** (5 mol %) ■; catalyst **3** (2.5 mol %) ▲; Jacobsen catalyst (5 mol %) ◇.

cyanide addition to α,β-unsaturated imides. In contrast, the increased crowding of catalytic units on the support lowers the selectivity and conversion (in the case of catalyst **1**) for the monometallic indole addition to α,β-unsaturated ketones. Catalyst **3** with the longest linker was found to enhance the bi- and monometallic reaction pathway. For the bimetallic pathway the longer linker facilitated salen–salen interaction in the transition state, while for the monometallic pathway, it improved solubility of the catalyst in the reaction medium leading to improved activities. Lastly the effect of the support flexibility was observed for the conjugate addition of tetrazoles for which significant enhancement of catalytic activity was observed with the optimal catalyst **3** relative to its non-supported analogue. Such a study that compares the effect of the support and linker on the catalytic activity of reactions which follow different mechanistic pathways paves the way for the rational design of highly active and selective supported catalysts.

Experimental Section

General: All starting materials were obtained from commercial suppliers and used without further purification unless otherwise stated. All air- or moisture-sensitive reactions were performed using oven-dried or flame-dried glassware under an inert atmosphere of dry argon or nitrogen. Air- or moisture-sensitive liquids and solutions were transferred by means of a syringe or cannula. Dichloromethane was distilled from calcium hydride, benzene from sodium, and 2-propanol from calcium sulfate.

CAUTION: Trimethylsilyl cyanide and hydrogen cyanide are highly toxic and should be handled extremely carefully in a fume hood as per the experimental protocol mentioned below.

Analytical thin-layer chromatography (TLC) was performed on Silica XHL pre-coated (250 μm thickness) glass-backed TLC plates from Sorbent Technologies. Eluting solvents are reported as volume ratios or volume percents. Compounds were visualized by using UV light or potassium permanganate stains. Flash column chromatography was performed with silica gel 60 Å (230–400 mesh). All ^{1}H and ^{13}C NMR spectra were recorded on Varian Mercury Vx 300 or Varian Mercury Vx 400 spectrometers with $CDCl_3$ as solvent. Chemical shifts are expressed in parts per million (δ), coupling constants (J) are reported in Hertz (Hz), and splitting patterns are reported as singlet (s), doublet (d), triplet (t), quartet (q), unresolved multiplet (m), and apparent (app). All NMR spectra are referenced using residual solvent peaks as the standard with δ values of 7.26 ppm for $CDCl_3$. High-resolution mass spectra were obtained from the Georgia Institute of Technology mass spectrometry lab. Gel-permeation chromatography (GPC) analyses were performed on a Waters GPC system with a Waters 1515 binary pump coupled with a Waters 2414 refractive index detector, and referenced to poly(styrene) standards. Methylene chloride was used as the mobile phase with a flow rate of 1.0 mL min^{-1}. Chiral HPLC analyses were performed on a Shimadzu-10 A system, using Pirkle-L-Leucine column from Regis Technologies or a Chiralcel OD column from Daicel Chemical Industries.

Salen ligand 4: (*R*,*R*)-1,2-Diaminocyclohexane monohydrochloride[27] (642 mg, 4.27 mmol, 1 equiv), methanol (22 mL), and some 4 Å molecular sieves were added to a flame dried 100 mL Schlenk flask equipped with a stir bar under an atmosphere of argon. Subsequently, 3,5-di-*tert*-butyl-2-hydroxybenzaldehyde (1.00 g, 4.27 mmol, 1 equiv) was added. The solution was allowed to stir for 3 h followed by the addition of 3-*tert*-butyl-2,5-dihydroxybenzaldehyde[10] (829 mg, 4.27 mmol, 1 equiv) as a solution in CH_2Cl_2 (22 mL) and NEt_3 (1.2 mL, 8.5 mmol, 2 equiv). The reaction mixture was stirred for an additional 3 h and then concentrated in vacuo to afford a brown residue. CH_2Cl_2 (200 mL) and water (200 mL) were added to the residue. The organic layer was separated and the aqueous layer was extracted with CH_2Cl_2 (2×100 mL). The combined organic layers were washed with water and saturated NaCl solution, dried over anhydrous magnesium sulfate, filtered, and concentrated in vacuo to afford a brown solid. The crude product was subjected to flash column chromatography (gradient elution: 10:1→5:1 hexane/EtOAc) to afford 1.6 g (74 %) of the salen **4** as a bright yellow solid. TLC R_f=0.35 (5:1 hexane/EtOAc); ^{1}H NMR (300 MHz, $CDCl_3$): δ=13.4 (brs, 2H; OH), 8.28 (s, 1H; N=C*H*), 8.18 (s, 1H; N=C*H*), 7.30 (d, J=2.5 Hz, 1H; H_{Ar}), 6.96 (d, J=2.5 Hz, 1H; H_{Ar}), 6.80 (d, J=3.0 Hz, 1H; H_{Ar}), 6.46 (d, J=3.0 Hz,1H; H_{Ar}), 3.29 (m, 2H; 2NC*H*CH$_2$), 1.98–1.86 (m, 4H; 2 C*H*$_2$), 1.74 (m, 2H; C*H*$_2$), 1.45 (m, 2H; C*H*$_2$), 1.41(s, 9H; C(C*H*$_3$)$_3$), 1.38 (s, 9H; C(C*H*$_3$)$_3$), 1.24 (s, 9H; C(C*H*$_3$)$_3$), 1.19 (s, 3H; C*H*$_3$), 1.19–1.24 (m, 2H; C*H*$_2$), 1.01–1.1 ppm (m, 2H; C*H*$_2$); ^{13}C NMR (75 MHz, $CDCl_3$): δ= 165.9, 164.9, 158.1, 154.4, 146.7, 140.2, 139.9, 138.5, 136.4, 126.9, 126.0, 118.3, 117.9, 117.7, 114.5, 72.4, 72.2, 60.5, 34.9, 34.8, 34.0, 33.15, 33.1, 31.4, 29.4, 29.2, 24.2, 14.2 ppm; HRMS (ESI$^+$) calcd for $C_{32}H_{47}N_2O_3$ [M+H]$^+$: 507.3581; found: 507.3547.

General procedure for the synthesis of salen cyclooctene esters: A solution of the salen ligand (1 equiv) in CH_2Cl_2 (0.13 M) was added to a flame dried round-bottom flask equipped with a magnetic stir bar and a reflux condenser. DCC (1.1 equiv), the appropriate cyclooctene derived alcohol (1 equiv), and DMAP (catalytic) were added to this solution. The reaction mixture was heated under reflux for 12 h under an atmosphere of Ar, following which the reaction mixture was diluted with CH_2Cl_2 and filtered. The filtrate was dried over magnesium sulfate, filtered, and concentrated in vacuo to afford a yellow solid. The crude mixture was subjected to flash column chromatography to afford the target product.

Salen cyclooctene ester **7**: Salen ligand **4** (500 mg, 0.987 mmol), acid **5**[10] (152 mg, 0.987 mmol), and DCC (204 mg, 0.987 mmol) were used. Flash chromatography (20:1 hexane/EtOAc) afforded 338 mg (58 %) of the product as a bright yellow solid. TLC R_f=0.43 (10:1 hexane/EtOAc); ^{1}H NMR (300 MHz, $CDCl_3$): δ=13.84 (s, 1H; OH), 13.63 (brs, 1H; OH), 8.30 (s, 1H; N=C*H*), 8.22 (s, 1H; N=C*H*), 7.31 (d, J=2.2 Hz, 1H;

H_{Ar}), 6.97 (d, J=2.4 Hz, 1H; H_{Ar}), 6.89 (d, J=2.6 Hz, 1H; H_{Ar}), 6.72 (d, J=2.0 Hz, 1H; H_{Ar}), 5.72 (m, 2H; C*H*=C*H*), 3.31 (m, 2H; 2NC*H*CH_2), 2.73–2.36 (m, 2H; C$H_{cyclooct}$), 2.27–2.08 (m, 4H; C$H_{(cyclooct)}$), 2.06–1.63 (m, 11H; C*H*, C$H_{2(cyclooct,cyclohex)}$), 1.45 (m, 2H; C$H_{2(cyclohex)}$), 1.41 (s, 9H; C-(CH_3)$_3$), 1.38 (s, 9H; C(CH_3)$_3$), 1.24 ppm (s, 9H; C(CH_3)$_3$); ^{13}C NMR (75 MHz, $CDCl_3$): δ=176.5, 165.9, 164.7, 158.0, 157.9, 141.7, 139.9, 138.4, 136.3, 130.7, 129.5, 126.9, 125.9, 122.6, 121.3, 118.2, 117.7, 72.4, 72.2, 43.2, 34.9, 34.8, 34.0, 33.1, 31.6, 31.5, 31.4, 29.5, 29.4, 29.1, 27.8, 25.9, 25.4, 24.7, 24.2 ppm; HRMS (ESI$^+$) calcd for $C_{41}H_{59}N_2O_4$ [M+H]$^+$: 643.4469; found: 643.451.

*Salen cyclooctene ester **8***:[10] Salen ligand **4** (500 mg, 0.987 mmol), acid **6**[35] (223 mg, 0.987 mmol), and DCC (204 mg, 0.987 mmol) were used. Flash chromatography (gradient elution: 20:1→5:1 hexane/EtOAc) afforded 650 mg (92%) of the product as a bright yellow solid. TLC R_f= 0.22 (10:1 hexane/EtOAc); ^{1}H NMR (300 MHz, $CDCl_3$): δ=13.89 (s, 1H; OH), 13.62 (brs, 1H; OH), 8.30 (s, 1H; N=C*H*), 8.22 (s, 1H; N=C*H*), 7.32 (d, J=2.5 Hz, 1H; H_{Ar}), 6.99 (d, J=2.5 Hz, 1H; H_{Ar}), 6.93 (d, J= 2.9 Hz, 1H; H_{Ar}), 6.78 (d, J=3.0 Hz, 1H; H_{Ar}), 5.7–5.6 (m, 2H; C*H*= C*H*), 4.87 (m, 1H; C*H*OCO) 3.33 (m, 2H; 2NC*H*CH_2), 2.81 (m, 2H; C$H_{2(linker)}$), 2.67 (m, 2H; C$H_{2(linker)}$), 2.4–2.05 (m, 2H; C$H_{cyclooct}$), 2.0–1.55 (m, 14H; C*H*, C$H_{2(cyclooct,cyclohex)}$), 1.45 (m, 2H; C$H_{2(cyclohex)}$), 1.42 (s, 9H; C(CH_3)$_3$), 1.39 (s, 9H; C(CH_3)$_3$), 1.25 ppm (s, 9H; C(CH_3)$_3$); ^{13}C NMR (75 MHz, $CDCl_3$): δ=171.6, 171.59, 166.1, 164.8, 158.4, 158.1, 141.7, 140.2, 138.8, 136.6, 130.1, 129.8, 127.1, 126.2, 122.9, 121.6, 118.4, 117.98, 76.4, 72.7, 72.4, 35.2, 35.1, 34.3, 33.9, 33.8, 33.5, 33.3, 31.6, 29.7, 29.67 (overlapping signals), 29.5, 29.4, 25.7, 25.0, 24.5, 22.5 ppm; HRMS (ESI$^+$) calcd for $C_{44}H_{63}N_2O_6$ [M+H]$^+$: 715.4681; found: 715.4639.

*Salen cyclooctene ester **12***: Salen ligand **11**[23] (241 mg, 0.381 mmol), acid **5**[10] (74 mg, 0.38 mmol), and DCC (79 mg, 0.38 mmol) were used. Flash chromatography (20:1 hexane/EtOAc) afforded 180 mg (61%) of the product as a bright yellow solid. TLC R_f=0.48 (10:1 hexane/EtOAc); ^{1}H NMR (300 MHz, $CDCl_3$): δ=13.73 (s, 1H; OH), 13.72 (brs, 1H; OH), 8.32 (s, 1H; N=C*H*), 8.30 (s, 1H; N=C*H*), 7.31 (d, J=2.4 Hz, 1H; H_{Ar}), 7.23 (d, J=2.3 Hz, 1H; H_{Ar}), 7.00 (d, J=2.4 Hz, 1H; H_{Ar}), 6.92 (d, J=2.2 Hz, 1H; H_{Ar}), 5.8–5.59 (m, 2H; C*H*=C*H*), 3.98 (t, J=6.6 Hz, 2H; C$H_{2(linker)}$), 3.33 (m, 2H; 2NC*H*CH_2), 2.48–2.29 (m, 3H; C$H_{cyclooct}$), 2.2–1.43 (m, 24H; C*H*, C$H_{2(cyclooct,cyclohex,linker)}$), 1.41 (s, 9H; C(C$H_3$)$_3$), 1.40 (s, 9H; C(C$H_3$)$_3$), 1.24 (s, 9H; C(C$H_3$)$_3$), 1.2 (s, 3H; C(C$H_3$)$_2$), 1.19 (s, 3H; C(C$H_3$)$_2$), 1.05 ppm (m, 2H; C$H_{2(linker)}$); ^{13}C NMR (75 MHz, $CDCl_3$): δ= 178.0, 166.0, 165.99, 158.2, 158.16, 140.1, 138.7, 136.6, 136.5, 130.7, 129.8, 127.3, 126.95, 126.91, 126.3, 118.1, 118.08, 72.6, 72.59, 64.6, 44.5, 43.7, 37.3, 37.2, 35.2, 35.1, 34.3, 33.6, 33.5, 31.9, 31.6, 30.1, 29.7, 29.6, 29.2, 29.17, 28.9, 28.1, 26.1, 25.97, 24.7, 24.6 (overlapping signals), 24.4 ppm; HRMS (ESI$^+$) calcd for $C_{50}H_{77}N_2O_4$ [M+H]$^+$: 769.5878; found: 769.5882.

General procedure for the synthesis of macrocyclic oligomeric salen: In a scintillation vial equipped with a magnetic stir bar, a solution of Grubbs' third-generation initiator (0.04 equiv) in deoxygenated CH_2Cl_2 was added to a solution of monomer (1 equiv) in deoxygenated CH_2Cl_2 (final solution concentration 0.1 M with respect to monomer). The reaction mixture was stirred at RT for 30 min, followed by the addition of a few drops of ethyl vinyl ether to quench the reaction. The reaction mixture was concentrated in vacuo and the resultant residue was purified by flash column chromatography to obtain the pure oligomeric product.

*Salen oligomer **9***:[10] Salen cyclooctene ester **7** (161 mg, 0.25 mmol) and Grubbs' third generation initiator (8.8 mg, 0.01 mmol) were used. Purification by flash column chromatography (gradient elution: 25:1→10:1 hexane/EtOAc) afforded 117 mg of the oligomer **9** (73%) as a bright yellow solid. TLC R_f=0.46 (5:1 hexane/EtOAc); ^{1}H NMR (300 MHz, $CDCl_3$): δ=13.89 (s, 1H; OH), 13.63 (brs, 1H; OH), 8.30 (s, 1H; N=C*H*), 8.24 (s, 1H; N=C*H*), 7.31 (d, J=1.0 Hz, 1H; H_{Ar}), 6.98 (d, J= 2.1 Hz, 1H; H_{Ar}), 6.89 (s, 1H; H_{Ar}), 6.74 (s, 1H; H_{Ar}), 5.6–5.3 (brm, 2H; C*H*=C*H*), 3.31 (brm, 2H; 2NC*H*CH_2), 2.53 (brm, 1H; C*H*CO_2), 2.4–1.4 (m, 18H; C*H*, C$H_{2(cyclooct,cyclohex)}$), 1.40 (s, 9H; C(CH_3)$_3$), 1.39 (s, 9H; C-(CH_3)$_3$), 1.24 ppm (s, 9H; C(CH_3)$_3$); ^{13}C NMR (75 MHz, $CDCl_3$): δ= 175.2, 166.1, 164.8, 158.3, 158.1, 141.7, 140.1, 138.7, 136.6, 132.5–128.7 (2C, multiple signals H*C*=*C*H), 127.1, 126.2, 122.9, 121.5, 118.4, 117.96, 72.7, 72.3, 45.3–43.2 (1C, multiple signals *C*HCO_2), 35.2, 35.1, 34.2, 33.5, 33.4, 32.1, 31.6, 30.8–30.2 (m), 29.7, 29.3, 27.6–26.8 (m), 24.5, 24.2 ppm; MS (MALDI-TOF) calcd for $(C_{41}H_{58}N_2O_4)_n$: m/z (%): 1285.9 (100) [M]$^+$ (n=2), 1928.4 (68) [M]$^+$ (n=3), 2570.9 (22) [M]$^+$ (n=4), 3213.4 (7) [M]$^+$ (n=5); GPC M_n=1300, M_w=1800, PDI=1.35.

*Salen oligomer **10***: Salen cyclooctene ester **8** (150 mg, 0.210 mmol) and Grubbs' third-generation initiator (7.4 mg, 0.008 mmol) were used. Purification by flash column chromatography (gradient elution: 20:1→3:1 hexane/EtOAc) afforded 133 mg of the oligomer **10** (89%) as a bright yellow solid. TLC R_f=0.23 (5:1 hexane/EtOAc); ^{1}H NMR (300 MHz, $CDCl_3$): δ=13.8 (brs, 2H; OH), 8.30 (s, 1H; N=C*H*), 8.22 (s, 1H; N= C*H*), 7.32 (d, J=2.6 Hz, 1H; H_{Ar}), 6.99 (d, J=2.4 Hz, 1H; H_{Ar}), 6.93 (d, J=2.7 Hz, 1H; H_{Ar}), 6.77 (d, J=2.9 Hz, 1H; H_{Ar}), 5.5–5.2 (brm, 2H; C*H*=C*H*), 4.91 (m, 1H; C*H*OCO), 3.33 (m, 2H; 2NC*H*CH_2), 2.82 (m, 2H; C$H_{2(linker)}$), 2.70 (m, 2H; C$H_{2(linker)}$), 2.2–1.3 (m, 18H; C*H*, C$H_{2(cyclooct, cyclohex)}$), 1.45 (m, 2H; C$H_{2(cyclohex)}$), 1.41 (s, 9H; C(C$H_3$)$_3$), 1.38 (s, 9H; C-(C$H_3$)$_3$), 1.24 ppm (s, 9H; C(C$H_3$)$_3$); ^{13}C NMR (75 MHz, $CDCl_3$): δ= 171.98, 171.6, 166.1, 164.8, 158.4, 158.2, 141.7, 140.2, 138.8, 136.6, 132–128 (2C, multiple signals H*C*=*C*H), 127.1, 126.2, 122.9, 121.5, 118.4, 117.98, 72.7, 72.4, 35.2, 35.1, 34.3, 33.5, 33.3, 31.6, 29.7, 29.5 (overlapping signals), 29.1, 28.6, 24.5, 22.5 ppm; MS (MALDI-TOF) calcd for $(C_{44}H_{62}N_2O_6)_n$: m/z (%): 1429.9 (100) [M]$^+$ (n=2), 2144.4 (75) [M]$^+$ (n=3), 2858.9 (18) [M]$^+$ (n=4), 3574.5 (5) [M]$^+$ (n=5); GPC M_n=1900, M_w=2500, PDI= 1.33.

*Salen oligomer **13***: Salen cyclooctene ester **12** (161 mg, 0.209 mmol) and Grubbs' third-generation initiator (7.4 mg, 0.008 mmol) were used. Purification by flash column chromatography (gradient elution: 25:1→10:1 hexane/EtOAc) afforded 125 mg of the oligomer **13** (78%) as a bright yellow solid. TLC R_f=0.5 (5:1 hexane/EtOAc); ^{1}H NMR (300 MHz, $CDCl_3$): δ=13.7 (brs, 2H; OH), 8.31 (s, 1H; N=C*H*), 8.30 (s, 1H; N= C*H*), 7.30 (d, J=2.5 Hz, 1H; H_{Ar}), 7.22 (d, J=2.4 Hz,1H; H_{Ar}), 7.00 (d, J=2.5 Hz, 1H; H_{Ar}), 6.91 (d, J=2.5 Hz, 1H; H_{Ar}), 5.4–5.2 (brm, 2H; C*H*=C*H*), 4.00 (brm, 2H; C$H_{2(linker)}$), 3.32 (brm, 2H; 2NC*H*CH_2), 2.1–1.3 (m, 27H; C*H*, C$H_{2(cyclooct,cyclohex,linker)}$), 1.40 (s, 9H; C(C$H_3$)$_3$), 1.396 (s, 9H; C(C$H_3$)$_3$), 1.23 (s, 9H; C(C$H_3$)$_3$), 1.19 (s, 3H; C(C$H_3$)$_2$), 1.18 (s, 3H; C-(C$H_3$)$_2$), 1.05 ppm (m, 2H; C$H_{2(linker)}$); ^{13}C NMR (75 MHz, $CDCl_3$): δ= 176.6, 166.0, 165.98, 158.2, 158.16, 140.1, 138.7, 136.6, 136.5, 130–129.5 (2C, multiple signals H*C*=*C*H), 127.3, 126.94, 126.9, 126.3, 118.1, 118.07, 72.6, 72.58, 64.6, 44.5, 45.3–43.2 (1C, multiple signals *C*HCO_2), 37.2 (overlapping signals), 35.2, 35.16, 34.2, 33.6, 33.55, 31.6 (overlapping signals), 30.1, 29.7, 29.65, 29.2, 29.1, 28.9, 28.1, 26.0, 25.97, 24.8 (overlapping signals), 24.6 ppm (overlapping signals); MS (MALDI-TOF) calcd for $(C_{50}H7_6N_2O_4)_n$: m/z (%): 1538.3 (100) [M]$^+$ (n=2), 2306.9 (67) [M]$^+$ (n=3), 3076.6 (15) [M]$^+$ (n=4), 3844.3 (3) [M]$^+$ (n=5); GPC M_n=1850, M_w=2600, PDI=1.39.

General procedure for the metalation of oligomeric salen: A solution of the oligomer (1 equiv) in CH_2Cl_2 (0.16 M) were added to a flame dried Schlenk flask (10 mL) equipped with a magnetic stirrer bar in an atmosphere of argon. A solution of diethyl aluminum chloride in toluene (1.8 M, 1 equiv) was added slowly to the reaction flask. The reaction mixture was allowed to stir for 3 h, following which the solvents were removed *in vacuo* to afford a yellow solid. The resultant solid was rinsed with hexane (3×1.5 mL) and dried to afford the metalated oligomeric catalyst.

*Oligomeric catalyst **1***: Oligomer **9** (100 mg, 0.156 mmol) and a solution of diethyl aluminum chloride in toluene (86.0 μL, 0.155 mmol) were used to afford 108 mg of catalyst **1** (99%) as a bright yellow solid. ^{1}H NMR (300 MHz, $CDCl_3$): δ=8.33 (brs, 1H; N=C*H*), 8.30 (brs, 1H; N=C*H*), 7.56 (s, 1H; H_{Ar}), 7.13 (s, 1H; H_{Ar}), 7.09 (s, 1H; H_{Ar}), 6.97 (s, 1H; H_{Ar}), 5.6–5.3 (brm, 2H; C*H*=C*H*), 3.74 (brm, 1H; NC*H*CH_2), 3.09 (brm, 1H; NC*H*CH_2), 2.53 (brm, 1H; C*H*CO_2), 2.8–1.3 (m, 18H; C*H*, C$H_{2(cyclooct,\ cyclohex)}$), 1.53 (brs, 18H; 2C(C$H_3$)$_3$), 1.31 ppm (s, 9H; C(C$H_3$)$_3$); ^{13}C NMR (75 MHz, $CDCl_3$): δ=175.3, 167.1, 164.7, 158.8, 158.5, 141.1, 140.7, 138.8 (overlapping signals), 132.5–129.7 (2C, multiple signals H*C*= *C*H) , 128.3, 126.6, 123.1 (overlapping signals), 118.6 (overlapping signals), 72.7 (overlapping signals), 45.3–43.2 (1C, multiple signals *C*HCO_2), 35.8, 35.4, 34.2, 33.5, 32.6 (overlapping signals), 31.6, 30.8–30.2 (m), 29.9, 29.7, 27.6–26.8 (m), 25.5, 23.8 ppm; ICP calcd (%): Al 3.8; found: Al 4.7.

*Oligomeric catalyst **2***: Oligomer **10** (110 mg, 0.154 mmol) and a solution of diethyl aluminum chloride in toluene (86.0 μL, 0.155 mmol) were used

to afford 110 mg of catalyst **2** (92%) as a bright yellow solid. ^{1}H NMR (300 MHz, $CDCl_3$): δ = 8.4–8.0 (br m, 2H; 2N=C*H*), 7.54 (s, 1H; H_{Ar}), 7.13 (d, 1H; H_{Ar}), 7.08 (s, 1H; H_{Ar}), 6.96 (s, 1H; H_{Ar}), 5.5–5.2 (br m, 2H; C*H*=C*H*), 4.9 (br m, 1H; C*H*OCO), 4.0–3.0 (br m, 2H; 2NC*H*CH_2), 2.82 (m, 2H; $CH_{2(linker)}$), 2.70 (m, 2H; $CH_{2(linker)}$), 2.2–1.2 (m, 20H; C*H*, $CH_{2(cyclooct,cyclohex)}$), 1.5 (s, 18H; 2C($CH_3$)$_3$), 1.3 ppm (s, 9H; C($CH_3$)$_3$); ^{13}C NMR (75 MHz, $CDCl_3$): δ = 172.1, 171.6, 165.4, 161.8, 143.6, 141.3, 140.6, 138.9, 138.7, 132–128 (2C, multiple signals HC=*C*H), 129.3, 128.5, 128.1, 125.5, 123.1, 118.6, 118.4, 74.5, 74.4, 35.8, 35.2, 34.3, 34.2 (overlapping signals), 31.6, 29.95, 29.7 (overlapping signals), 29.6, 28.7, 25.5, 23.97 ppm; ICP calcd (%): Al 3.5; found: Al 4.2.

*Oligomeric catalyst **3***: Oligomer **13** (123 mg, 0.160 mmol) and a solution of diethyl aluminum chloride in toluene (89 μL, 0.16 mmol) were used to afford 120 mg of catalyst **3** (90%) as a bright yellow solid. ^{1}H NMR (300 MHz, $CDCl_3$): δ = 8.4–8.2 (br m, 2H; 2N=C*H*), 7.54 (s, 1H; H_{Ar}), 7.47 (s, 1H; H_{Ar}), 7.1 (s, 1H; H_{Ar}), 7.9 (s, 1H; H_{Ar}), 5.5–5.3 (br m, 2H; C*H*=C*H*), 4.02 (br m, 2H; $CH_{2(linker)}$), 3.6–3.3 (br m, 2H; 2NC*H*CH_2), 2.6–1.0 (m, 27H; C*H*, $CH_{2(cyclooct,cyclohex,linker)}$), 1.52 (s, 18H; 2C($CH_3$)$_3$), 1.3 (s, 9H; C($CH_3$)$_3$), 1.26–1.23 (s, 6H; 2C($CH_3$)$_2$), 0.85 ppm (m, 2H; $CH_{2(linker)}$); ^{13}C NMR (75 MHz, $CDCl_3$): δ = 176.6, 166.7, 166.1, 165.0, 162.1, 158.2, 141.4, 137.8, 131.4, 131–129.5 (2C, multiple signals H*C*=*C*H), 128.8, 127.97, 126.9, 126.2, 118.4 (overlapping signals), 72.1 (overlapping signals), 64.6, 44.5, 45.3–43.2 (1C, multiple signals *C*HCO_2), 37.2 (overlapping signals), 35.8, 35.2, 34.3, 33.6, 33.2, 31.6 (overlapping signals), 30.1, 29.9, 29.65, 29.4, 29.2, 28.9 (overlapping signals), 26.0, 25.5, 24.9 (overlapping signals), 24.5 ppm (overlapping signals); ICP calcd (%): Al 3.3; found: Al 4.1.

General procedure for the cyanide addition reaction: The appropriate catalyst (0.013 mmol, 0.05 equiv) was added to a Schlenk tube (25 mL) and dried azeotropically with toluene (2×50 μL). Subsequently, imide **14** (50 mg, 0.26 mmol, 1 equiv), toluene (80 μL), and TMSCN (132 μL, 1.06 mmol, 4 equiv) were added to the flask. The reaction mixture was heated gently with a heat gun and immersed in an oil-bath at 45 °C, following which 2-propanol (81 μL, 1.06 mmol, 4 equiv) was added. The flask was sealed and allowed to stir for 18 h, following which the flask was vented into an aqueous solution of $FeSO_4$ to quench unreacted HCN gas. After allowing the HCN to bubble out for 5–10 min, the solvent was removed under vacuum. The crude reaction mixture was subjected to flash column chromatography with 3:1 (hexane/EtOAc) to afford the adduct **15** as a white solid.[20] Enantiomeric excess determined by chiral HPLC (Pirkle-L-Leucine, 5% ethanol/hexanes, 0.7 mL min^{-1}, 254 nm); TLC R_f = 0.14 (3:1 hexane/EtOAc); ^{1}H NMR (300 MHz, $CDCl_3$): δ = 8.88 (s, 1H; N*H*), 7.89 (dd, *J* = 8.0, 1.5 Hz, 2H; H_{Ar}), 7.64 (t, *J* = 7 Hz, 1H; H_{Ar}), 7.54 (t, *J* = 6.3 Hz, 2H; H_{Ar}), 3.47 (dd, *J* = 17.2 , 7 Hz, 1H; C*H*CN), 3.31 (m, 1H CNCHCH*H*); 3.2 (m, 1H; NCCHC*H*H), 1.45 ppm (d, 3H; *J* = 7.3 Hz, CH_3).

General procedure for the kinetic studies for the cyanide addition reaction: The addition reaction was divided into 5–6 NMR tubes. In each tube the appropriate catalyst, imide substrate (7.6 mg. 0.04 mmol, 1 equiv), and toluene (4 μL) were added. Each NMR tube was sealed with a septum and TMSCN (20 μL, 0.16 mmol, 4 equiv) and 2-propanol (12 μL, 0.16 mmol, 4 equiv) were added. The reaction was heated to 45 °C and quenched at the appropriate time by adding $CDCl_3$ (400 μL). The amount of product formation was calculated by adding a known amount of 1,1,2,2-tetrachloroethane (0.0075 mmol) in $CDCl_3$ (100 μL) to the NMR tube as a standard.

General procedure for indole addition reaction: The appropriate catalyst (0.0137 mmol, 0.1 equiv), ketone **16**[32] (20.0 mg, 0.137 mmol, 1 equiv), and toluene (650 μL) were added to a scintillation vial (3 mL) equipped with a magnetic stir bar. Indole **17** (27.0 mg, 0.206 mmol, 1.5 equiv) was added to the solution and the reaction was allowed to stir for 18 h. Subsequently, the reaction mixture was concentrated in vacuo and purified by flash column chromatography to afford the adduct **18**.[22] Enantiomeric excess determined by chiral HPLC (Chiralcel OD, 15% isopropanol/hexanes, 0.5 mL min^{-1}, 254 nm); TLC R_f = 0.46 (3:1 hexane/EtOAc); ^{1}H NMR (300 MHz, $CDCl_3$): δ = 7.92–7.85 (m, 1H; H_{Ar}), 7.75–7.65 (m, 1H; H_{Ar}), 7.6–7.2 (m, 5H; H_{Ar}), 7.15–7.05 (m, 2H; H_{Ar}), 3.75 (m, 1H; C*H*), 3.54 (dd, *J* = 16.3, 6.9 Hz, 1H; CH*H*CO), 3.38 (dd, , *J* = 16.2, 7.3 Hz, 1H;CHC*H*HCO), 2.38 (s, 3H; CH_3), 1.5 ppm (d, *J* = 7 Hz, 3H; CH_3); ^{13}C NMR (75 MHz, $CDCl_3$): δ = 200.3, 137.5, 135.7, 133.0, 130.6, 128.7, 128.4, 125.3, 120.9, 119.3, 119.2, 115.7, 110.7, 45.9, 27.5, 21.3, 12.3 ppm.

General procedure for the kinetic studies for the indole addition reaction: The appropriate catalyst (0.0137 mmol, 0.1 equiv), ketone **16** (20.0 mg, 0.137 mmol, 1 equiv), [D_8]toluene (650 μL), indole **17** (27.0 mg, 0.206 mmol, 1.5 equiv), and 1,1,2,2-tetrachloroethane (8 μL) were added to an NMR tube. NMR spectra were obtained at different time points and comparison of the integration of the product peaks with the tetrachloroethane peak was used to determine conversions.

General procedure for the tetrazole addition reaction: The appropriate catalyst, tetrazole **19** (24.0 mg, 0.167 mmol, 1.2 equiv), and toluene (700 μL) were added to a scintillation vial (3 mL) equipped with a magnetic stir bar. The appropriate α,β-unsaturated compound (0.137 mmol, 1 equiv) was added to the solution and the reaction was allowed to stir for 26 h. Subsequently, the reaction mixture was concentrated in vacuo and purified by flash column chromatography to afford the adduct **20**.

*Tetrazole adduct **20a***: TLC R_f = 0.46 (3:1 hexane/EtOAc); ^{1}H NMR (300 MHz, $CDCl_3$): δ = 8.17–8.1 (m, 2H; H_{Ar}), 8.0–7.95 (m, 2H; H_{Ar}), 7.65–7.55 (m, 1H; H_{Ar}), 7.52–7.4 (m, 5H; H_{Ar}), 5,71 (m, 1H; C*H*CH_2), 3.98 (dd, *J* = 17.9, 6.4 Hz, 1H; CHCH*H*), 3.6 (dd, *J* = 17.8, 6.9 Hz, 1H; CHC*H*H), 1.78 ppm (d, *J* = 6.5 Hz, 3H; CH_3); ^{13}C NMR (75 MHz, $CDCl_3$): δ = 196, 165.1, 136.4, 133.96, 130.5, 129.1, 129.0, 128.3, 127.7, 127.1, 56.6, 44.3, 21.3 ppm.

*Tetrazole adduct **20b***:[34] TLC R_f = 0.21 (3:1 hexane/EtOAc); ^{1}H NMR (300 MHz, $CDCl_3$): δ = 9.17 (br s, 1H; N*H*), 8.18–8.1 (m, 2H; H_{Ar}), 7.9–7.82 (m, 2H; H_{Ar}), 7.63–7.55 (m, 1H; H_{Ar}), 7.53–7.4 (m, 5H; H_{Ar}), 5,61 (m, 1H; C*H*CH_2), 4.07 (dd, *J* = 18.4, 9.7 Hz, 1H; CHCH*H*), 3.64 (dd, *J* = 18.4, 5.2 Hz, 1H; CHC*H*H), 1.77 ppm (d, *J* = 7 Hz, 3H; CH_3); ^{13}C NMR (75 MHz, $CDCl_3$): δ = 172.7, 166.1, 165.1, 133.8, 132.3, 130.4, 129.3, 129.0, 128.1, 127.7, 127.1, 56.3, 43.6, 21.3 ppm.

General procedure for the kinetic studies for tetrazole addition reaction: The appropriate catalyst, tetrazole **19** (24.0 mg, 0.167 mmol, 1.2 equiv), [D_8]toluene (700 μL), 1,1,2,2-tetrachloroethane (10 μL), and the α,β-unsaturated compound (0.137 mmol, 1 equiv) was added. Aliquots (20 μL) were removed from the reaction mixture at different time intervals and diluted with $CDCl_3$ (400 μL). NMR spectra were obtained at different time points and comparison of the integration of the product peaks with the tetrachloroethane peak was used to determine conversions.

Theoretical methods: Density functional theory (DFT), executed with the Jaguar suite of programs,[36] was used to compute the optimized singlet state structures of the AlCl–salen catalysts with the B3LYP functional[37–39] and the 6-31G* basis set. Frequency computations at the converged geometries were performed to ensure the structures corresponded to potential energy minima. Atomic charges were computed by fitting to the DFT electrostatic potential.[40–42]

Acknowledgements

This research is supported by the U.S. DOE Office of Basic Energy Sciences through the Catalysis Science Contract No. DE-FG02-03ER15459. M.W. gratefully acknowledges a Camille Dreyfus Teacher/Scholar Award and an Alfred P. Sloan Fellowship.

[1] C. Baleizão, H. Garcia, *Chem. Rev.* **2006**, *106*, 3987–4043.
[2] L. Canali, D. C. Sherrington, *Chem. Soc. Rev.* **1999**, *28*, 85–93.
[3] N. E. Leadbeater, M. Marco, *Chem. Rev.* **2002**, *102*, 3217–3274.
[4] A. Corma, H. Garcia, *Adv. Synth. Catal.* **2006**, *348*, 1391–1412.
[5] Q.-H. Fan, Y.-M. Li, A. S. C. Chan, *Chem. Rev.* **2002**, *102*, 3385–3466.
[6] R. Breinbauer, E. N. Jacobsen, *Angew. Chem.* **2000**, *112*, 3750–3753; *Angew. Chem. Int. Ed.* **2000**, *39*, 3604–3607.
[7] P. K. Dhal, B. B. De, S. Sivaram, *J. Mol. Catal. A* **2001**, *177*, 71–87.
[8] J. M. Notestein, A. Katz, *Chem. Eur. J.* **2006**, *12*, 3954–3965.

[9] H. Sellner, J. K. Karjalainen, D. Seebach, *Chem. Eur. J.* **2001**, *7*, 2873–2887.
[10] X. Zheng, C. W. Jones, M. Weck, *J. Am. Chem. Soc.* **2007**, *129*, 1105–1112.
[11] D. E. White, E. N. Jacobsen, *Tetrahedron: Asymmetry* **2003**, *14*, 3633–3638.
[12] N. Madhavan, C. W. Jones, M. Weck, *Acc. Chem. Res.* **2008**, *41*, 1153–1165.
[13] R. G. Konsler, J. Karl, E. N. Jacobsen, *J. Am. Chem. Soc.* **1998**, *120*, 10780–10781.
[14] L. Canali, E. Cowan, H. Deleuze, C. L. Gibson, D. C. Sherrington, *Chem. Commun.* **1998**, 2561–2562.
[15] T. S. Reger, K. D. Janda, *J. Am. Chem. Soc.* **2000**, *122*, 6929–6934.
[16] M. Holbach, M. Weck, *J. Org. Chem.* **2006**, *71*, 1825–1836.
[17] X. Zheng, C. W. Jones, M. Weck, *Adv. Synth. Catal.* **2008**, *350*, 255–261.
[18] B. B. De, B. B. Lohray, S. Sivaram, P. K. Dhal, *J. Polym. Sci. Part A* **1997**, *35*, 1809–1818.
[19] F. Minutolo, D. Pini, A. Petri, P. Salvadori, *Tetrahedron: Asymmetry* **1996**, *7*, 2293–2302.
[20] G. M. Sammis, E. N. Jacobsen, *J. Am. Chem. Soc.* **2003**, *125*, 4442–4443.
[21] G. M. Sammis, H. Danjo, E. N. Jacobsen, *J. Am. Chem. Soc.* **2004**, *126*, 9928–9929.
[22] M. Bandini, M. Fagioli, M. Garavelli, A. Melloni, V. Trigari, A. Umani-Ronchi, *J. Org. Chem.* **2004**, *69*, 7511–7518.
[23] N. Madhavan, M. Weck, *Adv. Synth. Catal.* **2008**, *350*, 419–425.
[24] M. Alvaro, C. Baleizao, E. Carbonell, M. El Ghoul, H. García, B. Gigante, *Tetrahedron* **2005**, *61*, 12131–12139.
[25] E. Thorn-Csányi, K. Ruhland, *Macromol. Chem. Phys.* **1999**, *200*, 1662–1671.
[26] E. Thorn-Csányi, K. Ruhland, *Macromol. Symp.* **2000**, *153*, 145–150.
[27] M. Holbach, X. Zheng, C. Burd, C. W. Jones, M. Weck, *J. Org. Chem.* **2006**, *71*, 2903–2906.
[28] See Experimental Section and Supporting Information for details.
[29] The data was highly reproducible provided the catalysts were stored in an atmosphere of argon at low temperatures.
[30] See theoretical methods and Supporting Information for details.
[31] Catalyst **2** with the medium linker was not tested as it led to adducts with lower enantioselectivities for the cyanide addition reaction.
[32] M. R. Pitts, J. R. Harrison, C. J. Moody, *J. Chem. Soc. Perkin Trans. 1* **2001**, 955–977.
[33] M. Bandini, M. Fagioli, P. Melchiorre, A. Melloni, A. Umani-Ronchi, *Tetrahedron Lett.* **2003**, *44*, 5843–5846.
[34] M. Gandelman, E. N. Jacobsen, *Angew. Chem.* **2005**, *117*, 2445–2449; *Angew. Chem. Int. Ed.* **2005**, *44*, 2393–2397.
[35] K. Breitenkamp, J. Simeone, E. Jin, T. Emrick, *Macromolecules* **2002**, *35*, 9249–9252.
[36] Jaguar 5.5, L. L. C. Schrödinger, Portland, OR, 1991–2003.
[37] A. D. Becke, *J. Chem. Phys.* **1993**, *98*, 5648–5652.
[38] C. Lee, W. Yang, R. G. Parr, *Phys. Rev. B* **1988**, *37*, 785–789.
[39] P. J. Stephens, F. J. Devlin, C. F. Chabalowski, M. J. Frisch, *J. Phys. Chem.* **1994**, *98*, 11623–11627.
[40] L. E. Chirlian, M. M. Francl, *J. Comput. Chem.* **1987**, *8*, 894–905.
[41] R. J. Woods, M. Khalil, W. Pell, S. H. Moffat, V. H. Smith, Jr., *J. Comput. Chem.* **1990**, *11*, 297–310.
[42] C. M. Breneman, K. B. Wiberg, *J. Comput. Chem.* **1990**, *11*, 361–373.

Received: August 5, 2008
Published online: December 19, 2008

